First International Conference on
Microchannels and Minichannels
April 24-25 2003, Rochester, New York, USA
ICMM2003-1044

MODELING OF SURFACE-FLUID ELECTROKINETIC COUPLING ON THE LAMINAR FLOW FRICTION FACTOR IN MICROTUBES

Brutin D. David.Brutin@polytech.univ-mrs.fr
Tadrist L. Lounes.Tadrist@polytech.univ-mrs.fr

Ecole Polytechnique Universitaire de Marseille : Laboratoire I.U.S.T.I. U.M.R. 6595
Technopôle de Château Gombert - 5, Rue Enrico Fermi - 13453 Marseille Cedex 13 - FRANCE

ABSTRACT

The present work's originality lies in the evidence of a non negligible effect of the fluid ions' and co-ions' interaction with the wall surface in a microtube. This study is based on the EDL theory (Electrical Double Layer) which is developed here for a circular geometry. High electrical surface potentials are taken into account for the present study; they induce the non-linearity of the problem's main equation (Poisson-Boltzmann equation). The electrical field is determined, then the velocity profile and finally the Poiseuille number. We show that even with the EDL effect taken into account, the Poiseuille number does not depend on the mean velocity. Our model agrees with the experimental results for high surface potentials (> 25 mV). This is found by comparing with experiments previously carried out with microtubes ranging from 530 to 50 µm.

INTRODUCTION

The liquid flow hydrodynamics in microtubes is a subject presently investigated by many authors. The objective of these studies is to provide an answer to the numerous and dispersed results concerning the friction factor of liquid flows in microtubes and microchannels. In many studies, gas flows in microtubes show that the rarefaction effect is the origin of such difference between experimental and theoretical results. This can be explained by the slip velocity at the wall surface. The Knudsen number which compares the free path length to the tube diameter is a pertinent indication of the rarefaction effect on the friction factor of a gas flow in a microtube. However for a liquid flow, the theory has been developed less. Furthermore, experimental studies are much more difficult to do due to technical difficulties induced by higher working pressures. The interaction of ions with water is of great importance in biological and chemical applications. In a recent study, Hribar & al. (2002) model ion solvation in water. Like Robinson & Stokes (1959) they evidenced the influence of ions on water properties. The separation distance between two ions in a solution is a good indicator of the ions' influence as detailed in Tab. 1.

Tab. 1: Separation distance between two ions in a 1:1 electrolyte solution at several concentrations (water molecule diameter: 15.4 pm).

1:1 Electrolyte solution concentration (mol/L)	10^{-4}	10^{-3}	10^{-2}	10^{-1}	1
Ion separation distance (pm)	2025	940	436	203	94
Ion separation distance in H_2O molecules	132	61	28	13	6

Several authors indicate that for concentrations over 0.02 M the ions' influence cannot be neglected. This is confirmed by the separation distance which reaches only 22 water-molecule diameters. The differences experimentally observed in the literature may have many explanations which are currently under discussion. Three effects may be proposed: the micro-polar fluid theory [Eringen, 1966], the micro-moment theory [Mingun, 1987], the electrokinetics effects [Rice, 1965]. We focus our attention on the electrokinetics

effects. This theory also called the Electrical Double Layer (EDL) theory originates with Rice & al. (1965). Since then, several authors have tried to use the EDL theory to explain experimental deviation from the Stokes flow theory. Mala & al. in 1999 did experiments with microtube diameters ranging from 50 to 254 μm and evidenced higher friction factors up to 15 %. They attribute this deviation to the electrokinetic interaction between their microtube surface in stainless steel and their fluid: water. In the present work, we detail the EDL theory for a circular geometry and high surface potentials. Then, comparisons with our experimental results are made.

MODELING BASIS

EDL Principle

The EDL effect is based on the microscale flow and electrostatic surface potential (Fig. 1). Every solid surface brings electrical charges and so has an electrical surface potential. If a liquid flows near the surface containing ions, they will be attracted (ions) to the surface or repulsed (counter ions). This attraction will be a function of the ion valence, the surface charge and the ion concentration. An ion concentration profile will appear. Ions will accumulate in a layer with a thickness of a few ions, also called the compact layer (1 nm); a thin layer which can reach a micrometer with an ion concentration gradient can appear and is called the diffusive layer.

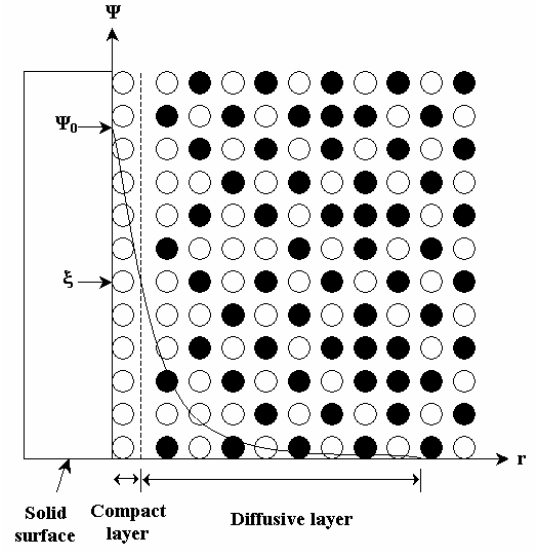

Fig. 1: Electrical Double Layer near a charged surface with ionic fluid

Assuming the surface is negatively charged, a large number of positive ions will be attracted to the surface and so few negative ions will be in the same space. The positive and negative ion concentration is given by Eq. (1) where n^+ and n^- are the positive ion concentration and the negative ion concentration in the capillary respectively (Fig. 2). The ion density can be expressed as a function of the electrostatic potential: Eq. (2).

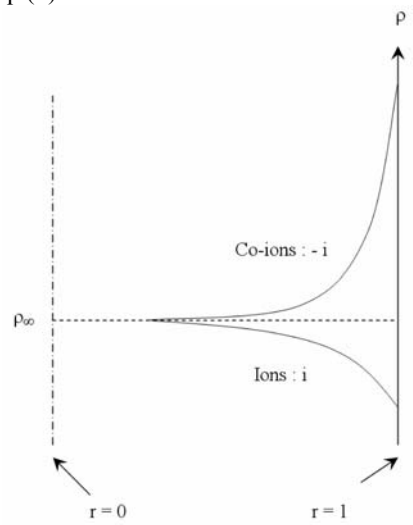

Fig. 2: Influence of ion and co-ion concentration due to a surface electrical potential.

$$\rho(r) = (n^+ - n^-)ze \qquad n^i = n_0 e^{-i\frac{ze\Psi(r)}{k_B T}} \tag{1}$$

$$\rho(r) = -2n_0 ze \sinh\frac{ze\Psi(r)}{k_B T} \tag{2}$$

The Poisson equation gives the relation between the electrical potential: ψ(r) and the charge density: ρ(r); in a circular geometry this relation is given in Eq. (3).

$$\frac{1}{r}\frac{d}{dr}(r\frac{d\Psi(r)}{dr}) = -\frac{4\pi}{\epsilon\epsilon_0}\rho(r) \tag{3}$$

For the purpose of mathematical calculation, we use dimensionless quantities. So, Eq. (2) and Eq. (3) give Eq. (5) and Eq.(6) respectively using the dimensionless parameters ($\bar{\psi}(r)$, $\bar{\rho}(r)$, $\bar{r}$) defined in Eq. (4).

$$\bar{\Psi} = \frac{e\Psi}{k_B T} \qquad \bar{\rho} = \frac{\rho}{n_0 e} \qquad \bar{r} = \frac{r}{R} \tag{4}$$

$$\bar{\rho}(\bar{r}) = -2\sinh\bar{\Psi}(\bar{r}) \tag{5}$$

$$\frac{1}{\bar{r}}\frac{d}{d\bar{r}}(\bar{r}\frac{d\bar{\Psi}(\bar{r})}{d\bar{r}}) = -\frac{4\pi n_0 e^2 R^2}{\epsilon\epsilon_0 k_B T}\bar{\rho}(\bar{r}) \tag{6}$$

By replacing $\bar{\rho}(r)$ from Eq. (5) into Eq. (6), we obtain the Poisson-Boltzmann equation: Eq. (7). κ is called the

electrokinetic dimensionless length and δ is the Debye-Huckel parameter, also called the Electric Double Layer thickness.

$$\frac{1}{\bar{r}}\frac{d}{d\bar{r}}(\bar{r}\frac{d\bar{\Psi}(\bar{r})}{d\bar{r}}) = \kappa^2 \sinh\bar{\Psi}(\bar{r}) \tag{7}$$

$$\kappa = \delta R = \sqrt{\frac{8\pi n_0 e^2}{\epsilon\epsilon_0 k_B T}}R \tag{8}$$

The boundary conditions of this non-linear second order differential equation are given in Eq. (9) where ξ is the electrostatic potential between the compact and the diffusive layer expressed in Volts. The determination of ξ will be dealt with a further section.

$$\begin{aligned} &\text{in } \bar{r}=0 \quad \Rightarrow \quad \frac{d\bar{\Psi}(\bar{r})}{dr}=0 \\ &\text{in } \bar{r}=1 \quad \Rightarrow \quad \bar{\Psi}(\bar{1})=\bar{\xi}=\frac{e\xi}{k_B T} \end{aligned} \tag{9}$$

Poisson-Boltzmann equation solution

The Poisson-Boltzmann equation cannot be solved directly. In almost all the literature, the main assumption is to consider a low surface electrostatic potential (ψ_0 < 25 mV) which induces the simplification in Eq. (10a) in the entire capillary. However, in recent experimental studies, it have been shown a higher surface potential with silicon surfaces of about 276 mV with de-ionized water for example and 107 mV with 10^{-4} M of KCl solution [Ren, 2001]. To solve the Poisson-Boltzmann equation without major simplification, we consider two regions in the capillary as described by Figs. 4 & 5. The hyperbolic sinus function is simplified using two functions of separate validity areas as indicated in Eqs. (10). Equation (10a) is used for the central region of the capillary where the potential $\overline{\psi}(r)$ is lower than 1 (ψ_0 < 25 mV) whereas Eq. (10b) is used near the wall where the potential surface is higher than 1 (ψ_0 > 25 mV).

$$\begin{aligned} &a) \quad if \quad \bar{\Psi}(\bar{r}) \ll 1 \quad \Rightarrow \quad \sinh(\bar{\Psi}(\bar{r})) \approx \bar{\Psi}(\bar{r}) \\ &b) \quad if \quad \bar{\Psi}(\bar{r}) \gg 1 \quad \Rightarrow \quad \sinh(\bar{\Psi}(\bar{r})) \approx \frac{1}{2}e^{\bar{\Psi}(\bar{r})} \end{aligned} \tag{10}$$

Fig. 3 shows the original hyperbolic sinus function compared to the two simplified functions.

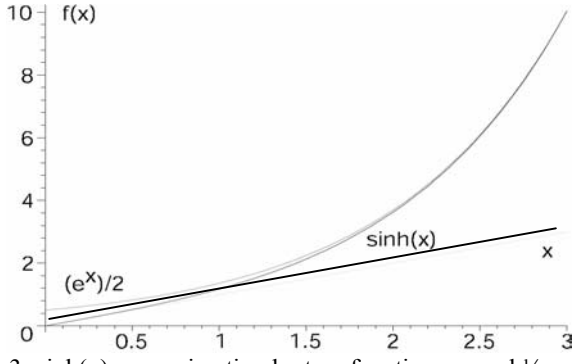

Fig. 3: sinh(x) approximation by two functions: x and ½ exp(x)

These are function of the location in the capillary; either one or the other will be used. The distance $\bar{r}$ = β is defined and satisfies $\overline{\psi}(\beta) = 1$. Thus, two potential functions are defined: $\overline{\psi}_1(\bar{r})$ when $\bar{r}$ < β and $\overline{\psi}_2(\bar{r})$ when $\bar{r}$ > β.

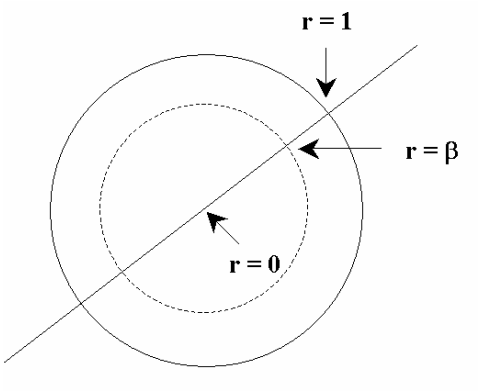

Fig. 4: A capillary cross-section.

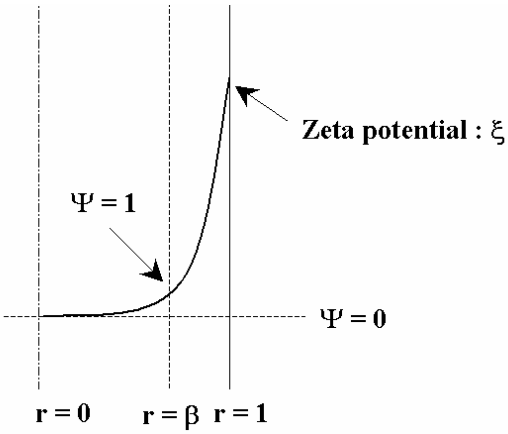

Fig. 5: A capillary length

The link conditions are the equality of both functions and derivatives at $\bar{r}$ = β are given in Eqs. (11).

$$\begin{aligned} \bar{\Psi}_1(\beta) &= \bar{\Psi}_2(\beta) \\ [\frac{d\bar{\Psi}_1(\bar{r})}{d\bar{r}}]_{\bar{r}=\beta} &= [\frac{d\bar{\Psi}_2(\bar{r})}{d\bar{r}}]_{\bar{r}=\beta} \end{aligned} \tag{11}$$

The boundary conditions are given in Eqs. (12).

$$\begin{aligned} &\text{in } \bar{r}=0 \Rightarrow \frac{d\bar{\Psi}_1(\bar{r})}{d\bar{r}}=0 \\ &\text{in } \bar{r}=1 \Rightarrow \bar{\Psi}_2(1)=\bar{\xi} \end{aligned} \tag{12}$$

The link condition of the potential function derivative will be used to obtain β. Due to the fact that β has no analytic

solution, we will use a numerical solver and will present only the numerical solution. Now the addition of a volume force due to the presence of ions in the fluid is possible.

Momentum equation modified

The momentum equation applied to the fluid is considered with a new volumic force due to the heterogeneous presence of ions: Eq. (13).

$$\mu \bigtriangledown_{\wedge} \bigtriangledown_{\wedge} \mathbf{V} + (\mathbf{V}.\bigtriangledown)\mathbf{V} + \bigtriangledown P = \mathbf{F} \qquad (13)$$

Considering a 1D incompressible fluid flow on z axis; thus Eq. (14) is obtained.

$$\frac{\mu}{r}\frac{d}{dr}(r\frac{dU_Z(r)}{dr}) - \frac{dP}{dz} + F_Z = 0 \qquad (14)$$

For simplification, we will take the following convention:

$$P_Z = -\frac{dP}{dz} \qquad (15)$$

also, F_Z is expressed as a function of the ion bulk density:

$$F_Z = E_Z \rho(r) \qquad (16)$$

where E_Z is the streaming field defined by $E_Z = E_S/L$. Eq. (14) is put in a dimensionless form using Eq. (17).

$$\bar{U} = \frac{U_Z}{U_0} \qquad \bar{r} = \frac{r}{R} \qquad (17)$$

U_0 is as a reference velocity which will be determined in a further section. In this way, Eq. (18) is obtained.

$$\frac{1}{\bar{r}}\frac{d}{d\bar{r}}(\bar{r}\frac{d\bar{U}(\bar{r})}{d\bar{r}}) + K_1 - \frac{K_2\bar{E}_S}{\kappa^2}\frac{1}{\bar{r}}\frac{d}{d\bar{r}}(\bar{r}\frac{d\bar{\Psi}(\bar{r})}{d\bar{r}}) = 0 \qquad (18)$$

where K_1, K_2 and $\overline{E}s$ are defined in Eqs. (19) and (20).

$$K_1 = \frac{P_Z R^2}{\mu U_0} \qquad K_2 = \frac{2n_0 e\xi R^2}{\mu U_0 L} \qquad (19)$$

$$\bar{E}_S = \frac{E_S}{\xi} \qquad (20)$$

Eq. (18) is modified in Eq. (21) to obtain the $\overline{U}(\bar{r})$ expression.

$$\frac{1}{\bar{r}}\frac{d}{d\bar{r}}(\bar{r}\frac{d}{d\bar{r}}(\bar{U} - \frac{K_2\bar{E}_S}{\kappa^2}\bar{\Psi})) + K_1 = 0 \qquad (21)$$

Eq. (21) spatially integrated two times gives Eq. (22).

$$\bar{U}(r) = \frac{K_1}{4}(1 - r^2) - \frac{K_2\bar{\xi}\bar{E}_S}{\kappa^2}(1 - \frac{\bar{\Psi}(r)}{\bar{\xi}}) \qquad (22)$$

The knowledge of the fluid velocity distribution in the capillary depends on the electrostatic potential knowledge through the second term of Eq. (22) but E_S, the streaming potential expression, is still unknown.

Streaming potential expression

The fluid flow imposed by a pressure gradient (the opposite of electro-osmotic flow) implies an electrical field called the streaming potential (E_S). The current due to the charge displacement in the flow is called the streaming current (I_S). The I_S expression is given by Eq. (23).

$$I_S = 2\pi \int_0^R U(r)\rho(r) r dr \qquad (23)$$

By doing typical non-dimensioning on U(r), ρ(r); the $\bar{I}s$ expression is given by Eq. (24).

$$\bar{I}_S = \frac{I_S}{U_0 R^2 n_0 e} = -4\pi \int_0^1 \bar{U}(\bar{r})\bar{\Psi}(\bar{r})\bar{r} d\bar{r} \qquad (24)$$

Due to the electrical neutrality of the fluid, a conduction current (I_C) appears in the fluid to balance the streaming current. It expression is given in Eq. (25).

$$I_C = \frac{E_S\lambda_0}{L}\int_0^R 2\pi r \cosh\bar{\Psi}(r) dr \qquad (25)$$

The dimensionless form of I_C is obtained using Eqs. (26) and gives Eq. (27)

$$\bar{L} = \frac{L}{R} \qquad \bar{E}_S = \frac{E_S}{\xi} \qquad (26)$$

$$\bar{I}_C = \frac{I_C}{\lambda_0 R\xi} = 2\pi\bar{E}_S\bar{L}\Sigma_1 \qquad (27)$$

where Σ_1 is given by Eq. (28).

$$\Sigma_1 = \int_0^1 \bar{r}\cosh\bar{\Psi}(\bar{r}) d\bar{r} \qquad (28)$$

$\overline{E}s$, which is given in Eq. (30) is obtained by the sum of the currents streaming and conduction in Eq. (29).

$$I_S + I_C = 0 \qquad (29)$$

$$\bar{E}_S = 2\frac{K_3}{\Sigma_1}\int_0^1 \bar{r}\bar{U}(\bar{r})\bar{\Psi}(\bar{r})d\bar{r} \tag{30}$$

where Σ_3 is given in Eq. (31).

$$K_3 = \frac{n_0 e L U_0}{\lambda_0 \xi} \tag{31}$$

Using the expression of the dimensionless streaming potential in the fluid velocity expression, it is now possible to given the Poiseuille number.

Poiseuille number expression

The Poiseuille number (Po) expression is based on the friction factor and so depends on the shear stress (τ_W) as explained by Eq. (32) where U_D is the mean fluid velocity and Re the mean Reynolds number defined in Eq. (33).

$$Po = fRe = \frac{4\tau_W}{\frac{1}{2}\rho_F U_D^2}Re \tag{32}$$

$$Re = \frac{2\rho_F U_D R}{\mu} \tag{33}$$

The shear stress expression is given by Eq. (34).

$$\tau_W = -\mu[\frac{dU}{dr}]_{r=R} = -\frac{\mu U_0}{R}[\frac{d\bar{U}}{d\bar{r}}]_{\bar{r}=1} \tag{34}$$

Equation (34) is injected into Eq.(32) and gives the relation between the Poiseuille number and the fluid velocity derivative: Eq. (35). Then using Eq. (22), we finally obtain Eq. (36).

$$Po = -16\frac{U_0}{U_D}[\frac{d\bar{U}}{d\bar{r}}]_{\bar{r}=1} \tag{35}$$

$$Po = 8\frac{U_0}{U_D}(K_1 + \frac{2K_2\bar{E}_S}{\kappa^2}[\frac{d\bar{\Psi}_2}{d\bar{r}}]_{\bar{r}=1}) \tag{36}$$

Now $\overline{Es}$ expression is known, but it is a function of $\bar{r}$ and K_1. K_1 is a function of the pressure gradient which is unknown. In a classical problem, the pressure gradient is fixed, and either the mass flow rate or the mean velocity can be deduced. Here both are required or their ratio without any assumption. β is determined using Eq. (11b). $\overline{Es}$ has been determined in the previous subsection, so U_D and K_1 are needed to express the Poiseuille number (Po). We proceed as in a classical tube to determine K_1 using the flow rate (Q_V) expression: Eq. (37).

$$Q_V = \int_0^R U(r)2\pi r dr \tag{37}$$

Q_V is put in a dimensionless form in Eq. (38).

$$\bar{Q}_V = \frac{Q_V}{\pi R^2 U_0} = 2\int_0^1 \bar{r}\bar{U}(\bar{r})d\bar{r} \tag{38}$$

U_D is the mean velocity, thus from the first equality of Eq. (37), we obtain: $\overline{Q_V} = U_D/U_0$. So using the second equality of Eq. (37) K_1 is extracted and gives Eq. (39) where Σ_2 is detailed in Eq. (40).

$$K_1 = 8[\frac{U_D}{U_0} + \frac{K_2\bar{E}_S}{\kappa^2}(1 - 2\Sigma_2)] \tag{39}$$

$$\Sigma_2 = \int_0^1 \bar{r}\bar{\Psi}(\bar{r})d\bar{r} \tag{40}$$

Eq. (39) is injected into Eq. (36) and gives Eq. (41).

$$Po = 64 + 16\frac{U_D}{U_0}\frac{K_2\bar{E}_S}{\kappa^2}[4 - 8\Sigma_2 + [\frac{d\bar{\Psi}_2}{d\bar{r}}]_{\bar{r}=1}] \tag{41}$$

Few remarks can be made concerning Eq. (41): without the EDL effect ($\overline{Es}$ = 0), we obtain: Po = 64. The mean velocity expression is still a problem. The solution is to choose the mean velocity as reference velocity. It allows a simplification and gives Eq. (42); now we have to show the Poiseuille number is not a function of the mean velocity even with the EDL effect. Eq. (40) gives Eq. (42) with $U_0 = U_D$.

$$Po = 64 + 16\frac{K_2\bar{E}_S}{\kappa^2}[4 - 8\Sigma_2 + [\frac{d\bar{\Psi}_2}{d\bar{r}}]_{\bar{r}=1}] \tag{42}$$

The expression between brackets can be easily calculated using the potential expression and is not a function of the velocity. K_2 and $\overline{Es}$ have to be detailed to show their product is not a function of U_D. Using Eq. (30), we inject the fluid velocity expression and obtain Eq. (43) where Σ_3 and Σ_4 are given by Eq. (44) and Eq. (45).

$$\bar{E}_S = \frac{K_1\Sigma_3}{\frac{2\Sigma_1}{K_3} + \frac{4K_2\bar{\xi}\Sigma_4}{\kappa^2}} \tag{43}$$

$$\Sigma_3 = \int_0^1 \bar{r}(1 - \bar{r}^2)\bar{\Psi}(\bar{r}) \tag{44}$$

$$\Sigma_4 = \int_0^1 \bar{r}(1 - \frac{\bar{\Psi}(\bar{r})}{\bar{\xi}})\bar{\Psi}(\bar{r}) \tag{45}$$

The new expression of $\bar{E}_S$ is function of K_1, K_2 and K_3: Eq. (46).

$$\bar{E}_S = f(K_1, K_3, \frac{1}{K_2}) = g(K_1, \frac{1}{U_D}, U_D) \qquad (46)$$

Using the K_2 expression given in Eq. (43), the Poiseuille number in Eq. (42) is shown not to be a function of the mean fluid velocity. So, it is possible to compute the Poiseuille number without the knowledge of the mean fluid velocity and the pressure gradient. This indicates that with an EDL effect the Poiseuille number is not a function of the Reynolds number. By fixing all the parameters, it will be possible in further section to numerically obtain the Poiseuille number.

CAPILLARY DIAMETER INFLUENCE

Principle

To test our model, we modify the capillary diameter and investigate the effect on the Poiseuille number's variation, by performing Poiseuille number measurements using a validated method [Brutin, 2003]. The capillary diameter's influence is experimentally investigated in a range of 530 to 50 µm using tap water. The relative surface roughness is also measured and evidences no effect on the fluid Poiseuille number due to the low value obtained under 2.10^{-4} for a 50 µm. The previous experimental results will be compared here to the model.

Experimental setup & data processing

The experimental setup is composed of a data acquisition system, capillaries, a balance and a pressure transducer. This experimental system allows accurate measurements even for low flow rates by preventing evaporation. Treated or untreated fused silica tubing made by Restek® is used. The data processing is based on a integration method fully detailed in a previous publication [Brutin, 2003].

Fluid parameters

We show the Poiseuille number is not a function of the fluid mean velocity, so for mathematical simplification we take $U_0 = U_D = 1$ m/s for further calculations. This value will provide partial results such as the shear stress which will be qualitatively correct but not quantitatively. For the tap water used, we have to determine the total number of ions per m^3. An analysis of the water is provided in Tab. 2. The sum of all the concentrations gives $C_0 = 7\ 10^{-3}$ M (mole/L) a number of ions per unit of volume (n_0) of:

$$n_0 = C_0 \mathcal{N} 10^{-3} = 4.21\ 10^{18}\ m^{-3}$$

where $\mathcal{N}$ is the Avogadro number. We take a room temperature of 295.15 K; and a relative permittivity of 80. A zeta potential or interfacial electrostatic potential (between the compact and the diffusive layer) must be taken before continuing. Considering the literature, for silicon surfaces with de-ionized water the surface potential has been measured at 276 mV and 107 mV using 10^{-4} M KCl solution [Ren, 2001]. For further calculation, we will take a zeta potential of 135 mV. In fact, this zeta potential has been obtained by iteration and is in the range of experimental potential measured by Ren & al. Thus $\bar{\xi}$ and the Debye-Huckel parameter can be calculated.

Tab. 2: Chemical composition of tap water given by decreasing concentrations (mole/L).

Ions	Concentration	Ions	Concentration
HCO_3^-	$2.8\ 10^{-3}$	K^+	$3.3\ 10^{-5}$
Ca^{2+}	$1.8\ 10^{-3}$	F^-	$4.2\ 10^{-6}$
SO_4^{2-}	$8.5\ 10^{-4}$	OH^-	$1.3\ 10^{-6}$
Cl^-	$5.8\ 10^{-4}$	Fe^{2+}	$5.4\ 10^{-7}$
Na^+	$5.4\ 10^{-4}$	Al^{3+}	$2.6\ 10^{-7}$
Mg^{2+}	$4.9\ 10^{-4}$	H_3O^+	$7.9\ 10^{-9}$
NO_3^-	$3.4\ 10^{-5}$		

$$\bar{\xi} = \frac{\xi e}{k_B T} = 5.3$$

$$\delta = \sqrt{\frac{8\pi n 0 e^2}{\epsilon * \epsilon_0 k T}} = 970721.28\ m^{-1}$$

Electrostatic potential functions

The potential function is here solved depending of $\bar{r}$: Eq. (47) & Eq. (48).

$$\frac{1}{\bar{r}} \frac{d}{d\bar{r}} (\bar{r} \frac{d\bar{\Psi}_1(\bar{r})}{d\bar{r}}) = \kappa^2 \bar{\Psi}_1(\bar{r}) \qquad \forall \bar{r} \in [0, \beta] \qquad (47)$$

$$\frac{1}{\bar{r}} \frac{d}{d\bar{r}} (\bar{r} \frac{d\bar{\Psi}_2(\bar{r})}{d\bar{r}}) = \frac{\kappa^2}{2} e^{\bar{\Psi}_2(\bar{r})} \qquad \forall \bar{r} \in [\beta, 1] \qquad (48)$$

The solution of Eq. (47) is easily obtained and given in Eq (49).

$$\bar{\Psi}_1(\bar{r}) = \frac{BesselI(0, \kappa\bar{r})}{BesselI(0, \beta\kappa)} \tag{49}$$

However, to obtain the solution of Eq. (48) few assumptions have to be made on two parameters (P & Q). A variable change is necessary (Levine, 1975). For our case: P < 0 which gives Eq. (50).

$$\bar{\Psi}_2(\bar{r}) = \ln\left(\frac{-P}{\kappa^2\bar{r}^2\cos^2(Q + \frac{1}{2}\sqrt{-P}\ln\bar{r})}\right) \tag{50}$$

with

$$P = [2 + \beta\kappa\frac{BesselI(1, \beta\kappa)}{BesselI(0, \beta\kappa)}]^2 - e^1\beta^2\kappa^2 \tag{51}$$

$$Q = \cos^{-1}\left(\sqrt{\frac{-P}{e^{\xi}\kappa^2}}\right) \tag{52}$$

In Fig. 6 the electrostatic potential function is plotted for all the range of capillary radii from 0 to 1 using Eq. (53).

$$\bar{\Psi}(\bar{r}) = \begin{cases} \bar{\Psi}_1(\bar{r}) = \frac{BesselI(0,\kappa\bar{r})}{BesselI(0,\beta\kappa)} & \text{si } \bar{r} \in [0,\beta], \\ \bar{\Psi}_2(\bar{r}) = \ln\left(\frac{-P}{\kappa^2\bar{r}^2\cos^2(Q+\frac{1}{2}\sqrt{-P}\ln\bar{r})}\right) & \text{si } \bar{r} \in [\beta,1], \end{cases} \tag{53}$$

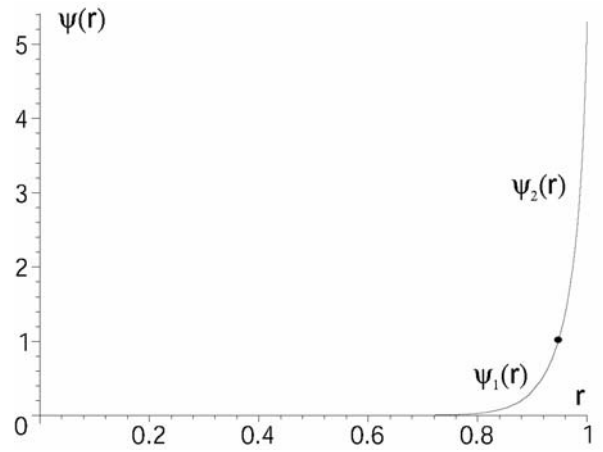

Fig. 6: Electrostatic potential function variation for a zeta potential of 135 mV and a capillary diameter of 60 µm.

So, from Eq. (53) the fluid velocity profile is determined and given in Eq. (54).

$$\bar{U}(\bar{r}) = \begin{cases} \bar{U}_1(\bar{r}) = \frac{K_1}{4}(1-\bar{r}^2) - \frac{K_2\bar{\xi}\bar{E}_S}{\kappa^2}(1 - \frac{\bar{\Psi}_1(\bar{r})}{\xi}) & \text{si } \bar{r} \in [0,\beta], \\ \bar{U}_2(\bar{r}) = \frac{K_1}{4}(1-\bar{r}^2) - \frac{K_2\bar{\xi}\bar{E}_S}{\kappa^2}(1 - \frac{\bar{\Psi}_2(\bar{r})}{\xi}) & \text{si } \bar{r} \in [\beta,1], \end{cases} \tag{54}$$

To plot a theoretical variation of the Poiseuille number with the EDL effect, a discretisation of the capillary diameter has to be done. For example, to compare our experimental results using tap water with the EDL model, computations have been done for capillary radii between 25 to 275 µm by step of 1 µm. The same increasing behavior is observed for decreasing capillary diameters. The differences can be explained by the model assumptions on the 1:1 electrolyte solution, the constant zeta potential.

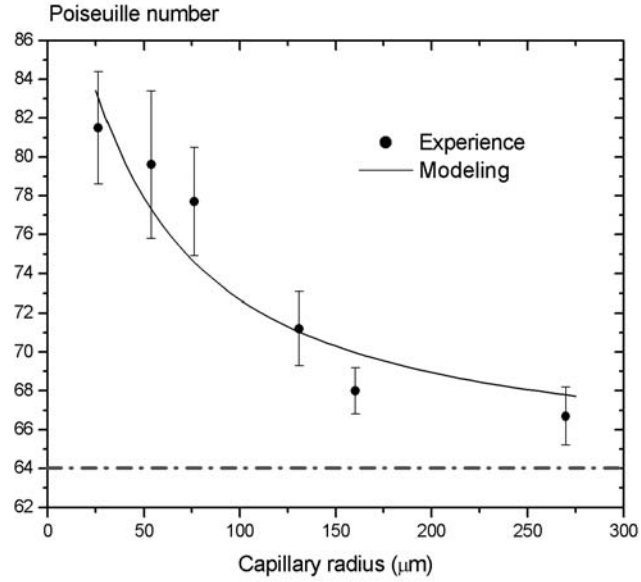

Fig. 7: Experimental versus modeling comparison for a zeta potential of 135 mV.

CONCLUSION & ON-GOING WORK

We developed here the Electrical Double Layer theory in a circular geometry with high surface potentials. It is shown that the Poiseuille number modified with the EDL effect does not depend on the Reynolds number as the Stokes flow theory for classical tubes. Furthermore, using a zeta potential according to the literature, it is shown that the experimental variation of the Poiseuille number for capillary decreasing diameters can be predicted by the theory. Further developments are currently being done on a second parameter as the ionic concentration to confirm the surface-fluid electrokinetic influence on the flow friction factor. Experiments with several concentrations of a 1:1 electrolyte salt solution (KCl) are conducted to evidence an influence of the fluid ionic concentration.

NOMENCLATURE

Roman Letters

n_0 Bulk concentration of ions (m^{-3})
k_B Boltzmann constant : $1.3805.10^{-23}$ $J.mol^{-1}.K^{-1}$

T	Temperature (°C)
R	Capillary radius (m)
r	Distance to the capillary center (m)
z	Ion valence
e	Charge of a proton : $1.6021.10^{-19}$ C
EDL	Electrical Double Layer
E_Z	Streaming potential ($V.m^{-1}$)
E_S	Electrical field (V)
L	Capillary length (m)
I_S	Streaming current (A)
I_C	Conduction current (A)
U_0	Reference velocity ($m.s^{-1}$)
U_D	Mean velocity ($m.s^{-1}$)
Po	Poiseuille number
N	Avogadro number: $6.0221.10^{23}$

Greek symbols

ε	Relative permittivity
ε_0	Static dielectric constant: $8.854.10^{-12}$ $C.V^{-1}.m^{-1}$
ρ	Local net electric charge density ($C.m^{-3}$)
ρ_F	Fluid density ($Kg.m^{-3}$)
ξ	Zeta potential (V)
ψ	Electrostatic potential (V)
β	Location which satisfy: $\psi(r) = 1$
δ	Debye-Huckel parameter (m^{-1})
κ	Dimensionless electrokinetic distance
μ	Fluid dynamic viscosity (Pa.s)
λ_0	Solid surface electrical conductivity ($\Omega.m^{-1}$)
τ_W	Wall strength (Pa)

REFERENCES

Mala G.M., Li D., Dale J. D., 1997, Heat transfer and fluid flow in microchannels, *Int. J. Heat Mass Transfer,* N°40, pp. 3079.

Kulinsky L., Wang Y., Ferrari M., 1999, *Electroviscous effects in microchannels*, *Proc. of SPIE - The International Society for Optical Engineering*, N°3606, pp. 158.

Pfund D., Rector D., Shekarriz A., Popescu A., Welty J., 2000, Pressure drop measurements in a microchannel, *Fluid Mechanics and Transport Phenomena,* N°46, pp. 1496.

Ren L., Qu W., Li D., 2001, Interfacial electrokinetic effects on liquid flow in microchannels, *Int. J. Heat and Mass Transfer,* N°44, pp. 3125.

Yang R.J., Fu L.M., Lin Y.C., 2001, Electroosmotic flow in microchannels, *J. Colloid and Interface Science*, N°239, pp. 98.

Weilin Q., Mala G.M., Dongqing L., 2000, Pressure-driven water flows in trapezoidal silicon microchannels, *Int. J. Heat Mass Transfer*, N°43, pp. 353.

Migun N.P., Prokhorenko P.P., 1987, Measurement of viscosity of polar liquids in microcapillaries, *Colloid Journal of the USSR*, N°49, pp. 894.

Eringen A.C., 1966, Theory of micropolar fluids, *J. Math. Mech*, N°16, 1966.

Pfahler J., Harley J., Bau H., Zemel J., 1990, Liquid transport in micron and submicron channels, *Sensors and Actuators*, N° 1, pp. 431.

Peng X.F., Peterson G.P., Wang B.X., 1994, Frictional flow characteristics of water flowing through rectangular microchannels, *Experimental Heat Transfer*, N°7, pp. 249.

Xu B., Ooi K.T., Wong N.T., Choi W.K., 2000, Experimental investigation of flow friction for liquid flow in microchannels, *Int. Comm. Heat Mass Transfers*, N°27, pp. 1165.

Mala G.M., Li D., 1999, Flow characteristics of water in microtubes, *Int. Journal of Heat and Mass Transfer*, N°20, pp. 142.

Idel'cik I., 1969, Memento des pertes de charge, *Eyrolles Ed. (Collection de la Direction des Etudes et Recherches d'Electricités de France)*, Part. 2, pp. 55.

Levine S., Marriott J.R., Neale G., Epstein N., 1975, Theory of electrokinetic flow in fine cylindrical capillaries at high zeta-potentials, *J. of Colloid and Interface Science,* N° 52, pp. 136.

Israelachvili J.N., 1991, Intermolecular & Surface forces, *2nd Edition Academic press*.

Kolpashchikov V.L., Mingun N.P., Prokhorenko P.P, 1983, Experimental determination of material micropolar fluid constants, *Int. J. of Engineering Science*, N° 21, pp. 405.

Rice C.L., Whitehead R., 1965, Electrokinetic flow in a narrow cylindrical capillary, *J. Physical Chemistry,* N° 69, pp. 4017.

Ma H.B., Peterson G.P., 1997, Laminar friction factor in microscale ducts of irregular cross section, *Microscale Thermophysical Engineering*, N° 1, pp. 253.

Van de Ven T.G.M., 2001, Electroviscous phenomena in colloidal dispersions, *Chemical Eng. Science,* N° 56, pp. 2947.

Brutin D., Tadrist L., 2003, Experimental friction factor of a liquid flow in microtubes, *Physics of Fluids*, Vol. 15, N° 3, pp. 653-661.

Robinson R., Stokes R.H., 1959, Electrolyte Solutions, *Butterworth Scientific Publications*, London.

Hribar B., Southall N.T., Vlachy V., Dill K.A., 2002, How Ions Affect the Structure of Water, *Journal of Chemical Society*, N° 124, pp. 12302-12311.